Stearne, *Eur. Polym. J.*, **1**, 227 (1965); (f) H. Inagaki, *Makromol. Chem.*, **86**, 289 (1965); H. Inagaki and T. Miyamoto, *ibid.*, **87**, 166 (1965); (g) D. Froelich, *J. Chim. Phys. Phys.-Chim. Biol.*, **64**, 1307 (1967).
(3) A. Dondos, P. Rempp, and H. Benoit, *Makromol. Chem.*, **130**, 233 (1969); (b) J. R. Urwin and M. Girolamo, *ibid.*, **160**, 133 (1972); (c) L. A. Utracki, R. Simha, and L. J. Fetters, *J. Polym. Sci., Part A-2*, **6**, 2051 (1968); L. A. Utracki and R. Simha, *Macromolecules*, **1**, 505 (1968); (d) H. Ohnuma, T. Kotaka, and H. Inagaki, *Polymer*, **10**, 501 (1969); (e) T. Kotaka, T. Tanaka, H. Ohnuma, Y. Murakami, and H. Inagaki, *Polym. J.*, **1**, 245 (1970); (f) T. Tanaka, T. Kotaka, and H. Inagaki, *ibid.*, **3**, 338 (1972).
(4) T. Kotaka, T. Tanaka, and H. Inagaki, *Polym. J.*, **3**, 327 (1972).
(5) T. Tanaka, Ph.D. Dissertation, Kyoto University, 1973.
(6) M. Leng and H. Benoit, *J. Polym. Sci.*, **57**, 263 (1962).
(7) J. Prud'homme and S. Bywater, *Macromolecules*, **4**, 543 (1971).
(8) H. Utiyama, K. Takenaka, M. Mizumori, and M. Fukuda, *Macromolecules*, **7**, 28 (1974).
(9) H. Utiyama, K. Takenaka, M. Mizumori, M. Fukuda, Y. Tsunashima, and M. Kurata, *Macromolecules*, **7**, 515 (1974).
(10) T. Tanaka, T. Kotaka, and H. Inagaki, *Macromolecules*, **7**, 311 (1974).
(11) See, for example, S. Windwer, "Markov Chains and Monte Carlo Calculations in Polymer Science", G. G. Lowry Ed., Marcel Dekker, New York, N.Y., 1970.
(12) (a) F. T. Wall and J. J. Erpenbeck, *J. Chem. Phys.*, **30**, 634, 637 (1959); (b) Z. Alexandrowicz, *ibid.*, **51**, 561 (1969); (c) Z. Alexandrowicz and Y. Accad, *ibid.*, **54**, 5338 (1971).
(13) (a) These values are based on an approximately correct distribution function. We have recerntly refined the model and obtained $\langle S^2 \rangle_A =$
(19) (a) P. J. Flory and T. G Fox, Jr., *J. Am. Chem. Soc.*, **73**, 1904 (1951); P. J. Flory, "Principles of Polymer Chemistry", Cornell University Press, Ithaca, N.Y., 1953; (b) T. A. Orofino and P. J. Flory, *J. Chem. Phys.*, **26**, 1067 (1957); (c) W. R. Krigbaum, *J. Am. Chem. Soc.*, **36**, 3758 (1954).
(20) E. Cohn-Ginsberg, T. G Fox, and H. F. Mason, *Polymer*, **3**, 97 (1962).
(21) M. Hattori, T. Tanaka, T. Kotaka, and H. Inagaki, to be published.
(22) J. B. Helms and G. Challa, *J. Polym. Sci., Part A-2*, **10**, 1447 (1972).
(23) (a) T. G Fox, *Polymer*, **3**, 111 (1962); (b) R. Kirste and G. V. Schultz, *Z. Phys. Chem. (Frankfurt am Main)*, **30**, 171 (1961).
(24) H. Yamakawa and G. Tanaka, *J. Chem. Phys.*, **47**, 3991 (1967).
(25) See, J. Brandrup and E. H. Immergut, Ed., "Polymer Handbook", 2d ed, Wiley-Interscience, New York, N.Y., 1975.
(26) P. J. Flory and W. R. Krigbaum, *J. Chem. Phys.*, **18**, 1086 (1950).
(27) T. Tanaka, T. Kotaka, and H. Inagaki, to be published.
$1.03\langle S^2 \rangle_{A,0}$ and $\langle G^2 \rangle = 2.54\langle G^2 \rangle_0$. See, T. Tanaka, T. Kotaka, and H. Inagaki, *Bull. Inst. Chem. Res., Kyoto Univ.*, in press. (b) J. Bendler and K. Šolc, private communication, 1975.
(14) D. Floelich and H. Benoit, *Makromol. Chem.*, **92**, 224 (1966).
(15) M. Leng and H. Benoit, *J. Polym. Sci., Part C*, **15**, 409 (1966).
(16) T. Tanaka and T. Kotaka, *Bull. Inst. Chem. Res., Kyoto Univ.*, **50**, 107 (1972).
(17) A. Ishihara, *J. Phys. Soc., Jpn.*, **5**, 201 (1950).
(18) H. Benoit and C. Wippler, *J. Chim. Phys. Phys.-Chim. Biol.*, **57**, 524 (1960); H. Benoit and D. Froelich, "Light Scattering from Polymer Solutions", M. B. Huglin, Ed., Academic Press, New York, N.Y. 1972.

Sedimentation Equilibrium of Polymers in Good Solvents

Petr Munk* and Michael E. Halbrook

Department of Chemistry, The University of Texas at Austin, Austin, Texas 78712.
Received November 25, 1975

ABSTRACT: A method of interpretation of sedimentation equilibrium data is developed, which is designed for the analysis of nonideal solutions. Only one equilibrium experiment is needed for each sample. The effect of heterogeneity is studied theoretically. The method is verified by measurement of polystyrene fractions in benzene and ethyl acetate; the equilibrium photographs being evaluated automatically. The method yields useful molecular weights and virial coefficients for the narrow fractions which were studied. For broader distributions caution is indicated.

In biochemistry, sedimentation equilibrium is the most frequently used method for the measurement of molecular weight. It requires only a minimum amount of sample and yields the molecular weight with good accuracy. The success of the method may be ascribed to the fact that a typical solution of biochemical interest is usually rather ideal; moreover, the systems under study are usually monodisperse, at worst, oligodisperse. However, several procedures were developed[1,2] for treatment of slightly nonideal oligodisperse system. These procedures consisted of point by point analysis of an equilibrium pattern in a single equilibrium run: the nonideality was approximately eliminated by using so-called "ideal" molecular weight moments and the data were analyzed with respect to their oligodispersity. Green and McKay[3] used (without any derivation) a method based also on point by point analysis which evaluates and eliminates the nonideality for highly nonideal homogeneous systems. Actually, their method is based on ideas, which are developed more broadly in the theoretical part of this paper.

The character of typical polymer solutions is rather different from that of biochemical solutions. All synthetic polymers are polydisperse; the polydispersity even of so-called narrow fractions or living polymers is rather broad in the terms of a biochemist. On top of that, many polymer solutions of interest exhibit strong nonideality. The main theoretical and experimental effort was devoted to pseudo-ideal theta solutions, for which the nonideality effect is eliminated. Several methods were devised for measuring various averages of molecular weight or even the complete molecular weight distribution function. Some of them[4-6] use a single equilibrium run, the others combine data from several runs.[6-8] Some authors, e.g., Adams et al.,[9] offer methods on how to correct the experimental data for the nonideality and then proceed with the analysis of the distribution function. Their method is based on auxiliary measurements (as light scattering, osmotic pressure).

For the analysis of nonideal polydisperse solutions the methods offered[8,10-12] require a substantial number of equilibrium runs at different original concentrations and rotor velocities. Characteristically, only one experimental point is derived from each equilibrium run.

In this paper, a method of interpretation of the experimental data is developed, which is based on point by point analysis of a single equilibrium pattern. The method is useful for strongly nonideal solutions and is an extension of the method of Munk and Cox,[13] which is applicable for moderately nonideal systems. The characteristic feature of the present method is that it eliminates the effects of nonideality *not* by extrapolating the experimental data to zero concentration but by drawing a tangent to an appropriate form of the experimental curve. The tangent yields a well-defined average of the molecular weight at the point where the tangent was drawn. Thus, in principle the point-by-point molecular weight average may be calculated and an insight into the polydispersity could be obtained. However, for narrow fractions, the experimental error does not allow for such detailed treatment. A single value is derived for the mid-cell and is believed to be a characteristic value for the whole original sample.

The method was used for measurement of five polystyrene samples with narrow distributions of molecular weight in

benzene (a highly nonideal solvent) and in ethyl acetate (a moderately nonideal solvent). Automatic evaluation of the equilibrium photographs[14] was used for acquisition of data points; the data were analyzed by a program written for the CDC 6600 computer.

Theoretical

The condition for equilibrium in an ultracentrifuge[15] for each component of the solute is

$$M_i(1 - \bar{v}_i\rho)\omega^2 r = \sum_k (\partial\mu_i/\partial c_k)_{T,p,c_j} (dc_k/dr) \quad (1)$$

which for a homogeneous solute reduces to

$$M_2(1 - \bar{v}_2\rho)\omega^2 r = (\partial\mu_2/\partial c_2)_{T,p} (dc_2/dr) \quad (2)$$

Here, index 1 refers to the solvent, index 2 to the homogeneous solute, and indices i, j, k to the components of heterogeneous solute. M_i, $\bar{v}_i$, μ_i, and c_i are respectively the molecular weight, partial specific volume, chemical potential, and concentration (in g/ml units) of the ith component. The distance from the rotational axis is r, ω is the angular velocity of the rotor, ρ is the density of the solution, p is the pressure, and T is the absolute temperature. In the relations applying to heterogeneous solutes, $c = \Sigma_i c_i$ will be the total concentration of solutes.

Homogeneous Solute

It is convenient to express the chemical potentials in a way compatible with the virial expansion of the osmotic pressure,

$$\mu_1 - \mu_1^0 = \bar{V}_1\pi \quad (3)$$

$$\pi/c_2RT = 1/M_2 + A_2c_2 + gA_2^2M_2c_2^2 = (1/M_2)(1 + \Gamma_2c_2 + g\Gamma_2^2c_2^2 + \ldots) \quad (4)$$

Here, $\bar{V}_i = M_i\bar{v}_i$ is the partial molar volume of the ith component, R is the gas constant, A_2 is the second virial coefficient, $\Gamma_2 = A_2M_2$, and g is a numerical factor[16,17] with a value of about $\frac{1}{4}$. In order to simplify the subsequent calculations we assume that the partial molar volumes are constants independent of the composition of the system; i.e., the volume changes in mixing are neglected. The density of the solution is then related to the density of the pure solvent ρ_1 and to the concentration by means of a convenient expression

$$(1 - \bar{v}_2\rho) = (1 - c_2\bar{v}_2)(1 - \bar{v}_2\rho_1) \quad (5)$$

The derivative of the chemical potential of the solute is now obtained from eq 3 and the Gibbs–Duhem relation as

$$(\partial\mu_2/\partial c_2)_{T,p} = RT(1 - c_2\bar{v}_2)(1/c_2 + 2A_2M_2 + 3gA_2^2M_2^2c_2 + \ldots) \quad (6)$$

Finally, by integration of (6) we get

$$\mu_2 - \mu_2^0 = RT[\ln c_2 - c_2\bar{v}_2 + 2A_2M_2c_2(1 - c_2\bar{v}_2/2) + 3gA_2^2M_2^2c_2^2(1 - 2c_2\bar{v}_2/3)/2 + \ldots] \quad (7)$$

Here, the reference chemical potential, μ_2^0, is defined in such a way that the logarithm of the activity coefficient (which is represented by all the terms on the right-hand side of eq 7 except the first one) vanishes at the limit of zero concentration. Returning to the sedimentation equilibrium we substitute eq 5 and 6 into eq 2 and get

$$1/M_{App} \equiv (1 - \bar{v}_2\rho_1)\omega^2c_2r/RT\ (dc_2/dr) = 1/M_2 + 2A_2c_2 + 3gA_2^2M_2c_2^2 + \ldots = 1/M_2[1 + 2\Gamma_2c_2 + 3g\Gamma_2^2c_2^2 + \ldots] \quad (8)$$

According to eq 8, the molecular weight of the solute is obtained by extrapolation of the M_{App}^{-1} value to vanishing concentration of the solute. The concentration of the solute varies along the cell, hence, the dependence of M_{App}^{-1} on concentration may be constructed from a single equilibrium experiment. When the nonideality is only moderate ($\Gamma_2c_2 \leq 0.1$) linear extrapolation yields the proper value of M_2 as shown by Munk and Cox.[13] However, for more nonideal solutions, the quadratic term in eq 8 is not negligible; the extrapolation should be done along a curved line that would introduce an appreciable uncertainty.

A similar situation exists in the analysis of osmotic data. As Berglund[18] first suggested, osmotic data yield an almost straight line when plotted as $(\pi/c_2)^{1/2}$ vs. c_2. This results from the fact that, for the special case $g = \frac{1}{4}$, the first three terms of eq 4 may be written as

$$(\pi/c_2RT)^{1/2} = (1/M_2)^{1/2}[1 + \Gamma_2c_2/2] \quad (9)$$

According to light-scattering theory, the reduced reciprocal intensity of the light scattered by nonideal solutions is proportional to the expression given in brackets in eq 8. If the parameter g has a physically reasonable value $\frac{1}{3}$ then the expression in brackets is a full square $[1 + \Gamma_2c]^2$. It was suggested by Flory[19] and verified by Berry[20] that the square-root plot of the light-scattering data would be more linear and thus yield better results.

Consequently, it is proposed to plot the data for sedimentation equilibrium in a similar way, namely, $M_{App}^{-1/2}$ vs. c_2. The intercept is then equal to $M_2^{-1/2}$, Γ_2 is equal to the slope divided by the intercept, and A_2 is equal to the slope multiplied by the intercept.

Heterogeneous Solute

Heterogeneity of the solute influences the analysis of the sedimentation equilibrium data in several ways. (1) The second virial coefficient A_2 is a function of the molecular weight. (2) A_2 is a measure of the interaction of two molecules of the same weight; the interaction coefficient for molecules of different weights is not properly known. (3) The redistribution of the mass caused by sedimentation is different for each component of the solute, i.e., the molecular weight distribution of the polymer varies along the cell. (4) Due to this variation, extrapolation of the experimental data beyond the cell boundaries (i.e., to vanishing concentration) does not correspond to any physical situation and should be avoided. It should be noted that the redistribution also depends on the length of the solution column and on the velocity of the rotor.

In the following section we will analyze the sedimentation equilibrium of a model system defined in such a way as to circumvent some of the difficulties mentioned above. Thus, our heterogeneous model will have a relatively narrow unimodal distribution of molecular weight, say $\bar{M}_w/\bar{M}_n \approx \bar{M}_z/\bar{M}_w < 1.2$. Here $\bar{M}_n$, $\bar{M}_w$, and $\bar{M}_z$ are respectively the number, weight, and z averages of molecular weight, defined in the usual way. The second virial coefficient, A_2, and the partial specific volume of the solute, $\bar{v}_2$, will be considered as constants independent of molecular weight. Then the chemical potential of the ith component of the solute will be postulated in analogy to eq 7 as

$$\mu_i - \mu_i^0 = RT[\ln c_i - c\bar{v}_2 + 2A_2M_ic(1 - c\bar{v}_2/2) + 3gA_2^2M_i^2c^2(1 - 2c\bar{v}_2/3)/2 + \ldots] \quad (10)$$

Moreover, when appropriate, the value $g = \frac{1}{3}$ will be substituted, i.e., the value which linearized the square-root plot for homogeneous solute. Using the Gibbs–Duhem relation, we may now calculate the osmotic pressure as

$$\pi/cRT = 1/\bar{M}_n + A_2c + gA_2^2\bar{M}_wc^2 + \ldots \quad (11)$$

Differentiating eq 10 with respect to c_k we obtain the partial derivatives needed in eq 1 as

$$(\partial\mu_i/\partial c_k)_{T,p,c_j} = RT[\delta_{ik}/c_i - \bar{v}_2 + (1 - c\bar{v}_2)(2A_2M_i + 3gA_2^2M_i^2c + \ldots)] \quad (12)$$

Here, δ_{ik} has the value of 1 for $i = k$ and value of 0 for $i \neq k$. Substituting eq 5 (with c replacing c_2) and eq 12 into eq 1, multiplying by c_i, and summing over i, we get after slight rearrangement

$$1/M_{App} = 1/\bar{M}_w + 2A_2c + 3gA_2^2c^2\bar{M}_z + \ldots \quad (13)$$

in analogy to eq 8. However, in eq 13 the molecular weight averages are functions of the position in the cell and, therefore, functions of concentration. To appreciate the effect of the redistribution we will calculate $d\bar{M}_w/dc$. The derivative can be obtained after some manipulation from eq 1 and 12 as

$$d\bar{M}_w/dc = (1 - c\bar{v}_2)[(\bar{M}_z - \bar{M}_w)/c - 3gA_2^2c\bar{M}_z\bar{M}_w(\bar{M}_{z+1} - \bar{M}_z) + \ldots] \quad (14)$$

$$d\bar{M}_w/dc \doteq (\bar{M}_w/c)(\bar{M}_z/\bar{M}_w - 1)(1 - A_2^2c^2\bar{M}_z^2) \quad (15)$$

In eq 14 and 15 all the molecular weight averages are functions of the position in the cell. The approximate relation 15 was obtained from eq 14 realizing that in a typical sedimentation experiment $c\bar{v}_2$ is negligible when compared to unity and that for narrow distributions $\bar{M}_{z+1}/\bar{M}_z \approx \bar{M}_z/\bar{M}_w$. The parameter g was set equal to $\frac{1}{3}$. It is apparent, that the change of the molecular weight average along the cell gets smaller as the value of $A_2c\bar{M}_z$ gets larger. (Note that the derivative should not become negative even for values of $A_2c\bar{M}_z$ larger than unity because the higher terms in the virial expansion eq 4, which would appreciably contribute in this region, were neglected.) Thus, the largest variation of $\bar{M}_w$ exists for the ideal solution ($A_2 = 0$). Assuming that the ratio $\bar{M}_z/\bar{M}_w$ does not vary much along the cell we may integrate eq 15 between the top and the bottom of the cell (superscripts t and b, respectively) to obtain for an ideal solution

$$\ln(\bar{M}_w^b/\bar{M}_w^t) = (\bar{M}_z/\bar{M}_w - 1)\ln(c^b/c^t) \quad (16)$$

Thus, for a typical experimental ratio $c^b/c^t = 4$ and a polymer fraction with $\bar{M}_z/\bar{M}_w = 1.2$ the ratio $\bar{M}_w^b/\bar{M}_w^t$ is 1.32 for an ideal solvent and less than that for a good solvent.

Let us now return to the analysis of eq 13. It is obvious from the above discussion that the extrapolation of the $1/M_{App}$ or $1/M_{App}^{1/2}$ to vanishing concentration (even if technically feasible) would lead to a region of concentrations where the molecular weight distribution of the polymer and its $\bar{M}_w$ are grossly different from the original sample and therefore it would yield values of little interest.

Instead, a different procedure is proposed: to draw a tangent to the dependence of either $1/M_{App}$ or $1/M_{App}^{1/2}$ on concentration. The tangent to the dependence $1/M_{App}$ vs. c is meaningful only if the third virial term in eq 13 is completely negligible ($A_2c\bar{M}_w < 0.15$). In that case, it is easy to show that the intercept, i, and slope, s, of the dependence $1/M_{App}$ vs. c are given by the following relations

$$i = (\bar{M}_z/\bar{M}_w^2)[1 - c\bar{v}_2(1 - \bar{M}_w/\bar{M}_z)] \quad (17)$$

$$s = 2A_2 - (1 - c\bar{v}_2)(\bar{M}_z/\bar{M}_w - 1)/c\bar{M}_w \quad (18)$$

The second term in brackets of eq 17 is completely negligible with respect to unity; thus the inverse intercept is equal to $\bar{M}_w^2/\bar{M}_z$, which for narrow fractions is close to the number average molecular weight, $\bar{M}_n$. The slope of the dependence is a measure of the second virial coefficient, A_2. However, the second term in eq 18 is not negligible; it increases with increasing heterogeneity, decreasing concentration, and decreasing molecular weight. For example, the second virial coefficient, A_2, estimated as half of the slope would be too low by 2.5×10^{-4} ml mol/g^2 for a sample with $\bar{M}_w = 100\,000$; $\bar{M}_z/\bar{M}_w = 1.2$; and $c = 0.004$ g/ml. When the third virial term in eq 13 is not negligible ($A_2c\bar{M}_w > 0.15$) both the molecular weight and virial coefficient estimated from the above plot would be too high.

In such a case a plot of $1/M_{App}^{1/2}$ vs. c is indicated. The computations are rather tedious in this case; the slope, s, and the intercept, i, are best represented by approximate relations 19–21.

$$i \doteq [(\bar{M}_z + \bar{M}_w)/2\bar{M}_w^{3/2}][1 - A_2c\bar{M}_w(\bar{M}_z - \bar{M}_w)/(\bar{M}_z + \bar{M}_w) + \ldots] \quad (19)$$

$$s \doteq A_2\bar{M}_w^{1/2}[1 + A_2c(\bar{M}_z - \bar{M}_w) + \ldots] - (\bar{M}_z - \bar{M}_w)/2c\bar{M}_w^{3/2}(1 + A_2c\bar{M}_w) + \ldots \quad (20)$$

$$is \doteq A_2[1 + (\bar{M}_z - \bar{M}_w)^2/2\bar{M}_w(\bar{M}_z + \bar{M}_w) + A_2c\bar{M}_z(\bar{M}_z - \bar{M}_w)/(\bar{M}_z + \bar{M}_w) + \ldots] - (\bar{M}_z + \bar{M}_w)(\bar{M}_z - \bar{M}_w)/4c\bar{M}_w^3(1 + A_2c\bar{M}_w) \quad (21)$$

During the derivation of relations 19–21 the parameter g was set equal to $\frac{1}{3}$. The neglected terms in higher powers of $A_2c\bar{M}_w$ tended to compensate the leading correction terms. The molecular weight calculated as a square of the inverse intercept represents the expression $4\bar{M}_w^3/(\bar{M}_w + \bar{M}_z)^2$; it is a value between the number average and the weight average of molecular weight (probably close to the weight average). For heterogeneous samples the nonideality introduces some error; for highly nonideal solutions ($A_2c\bar{M}_w \sim 1$) and $\bar{M}_z/\bar{M}_w = 1.2$ the molecular weight may be 20% too high, but usually the error is much less. When the second virial coefficient is calculated from the product of the slope and the intercept, is, the heterogeneity introduces an error comparable to the corresponding error in the plot of $1/M_{App}$ vs. c.

In summary, the two plots give comparable results for samples with moderate nonideality ($A_2c\bar{M}_w \leq 0.15$). For stronger nonideality only the square-root plot is applicable. The useful range for the latter plot is up to concentrations where the fourth virial term is important. Heterogeneity introduces additional correction terms; nevertheless we believe that the method is applicable up to values of $A_2c\bar{M}_w = 0.8$–1.0 or even higher for narrow fractions. The heterogeneity has almost no effect on estimated molecular weight at moderate nonidealities and a moderate effect at large nonidealities. However, its effect on the estimated value of A_2 may be rather significant especially when the virial coefficient is small. The absolute value of the error (and more the relative value) decreases with increasing nonideality.

It should be noted that the above analysis describes the tangent at any arbitrary point in the plot. Thus, at least in principle, the molecular weight averages could be estimated as a function of the position in the cell and the redistribution of the solute and its heterogeneity deduced from such a function. In practice, however, the experimental precision does not warrant such a treatment. Usually the whole dependence for a narrow fraction may be represented by a straight line within an experimental error. That applies to both types of plots. Such a straight line may be considered as a tangent at some point in the mid-cell. The molecular weight distribution in the mid-cell is quite close to the distribution of the original sample. It seems, therefore, reasonable to interpret the result obtained in this way as pertaining to the original whole sample.

Experimental Section

Polystyrene samples were obtained from Pressure Co., Pittsburgh, Pa. The ratio of molecular weights $\bar{M}_w/\bar{M}_n$ was claimed by the manufacturer to be less than 1.06 for the samples designated as **7b, 4b, 1c;** less than 1.10 for sample **3b,** and less than 1.15 for the high molecular weight sample **13a.**

Solvents. Reagent grade benzene and ethyl acetate were used without further purification.

Partial molar volume of polystyrene at 20 °C was repeatedly measured by A. Paar Precision Density Meter DMA 02C. The accepted value for solutions in benzene was 0.914 ml/g; for solutions in

ethyl acetate it was 0.916 ml/g. The solvent density at 20 °C was 0.8791 g/ml for benzene and 0.9006 g/ml for ethyl acetate.

Intrinsic viscosities were measured at 20 °C by an automatic viscometer Fica Viscomatic marketed by Bausch and Lomb.

Equilibrium experiments were performed at 20 °C in a Spinco Model E ultracentrifuge equipped with an electronic speed control. Heavy rotors AN-H and AN-J were employed. The cell was equipped with a Kel F coated aluminum double-sector centerpiece (12 mm) and sapphire windows. The concentration of polystyrene was between 0.006 (lowest molecular weight sample) and 0.004 g/ml (highest molecular weight). The sectors were filled respectively with 0.10 ml of solution and solvent. The velocity of the rotor was adjusted to produce the fringe pattern with the desired steepness of fringes. The rotor was kept at speed for 45–75 h; the longer times were used for higher molecular weight samples. Several interference and schlieren photographs were taken at different times; only the interference data were used in calculations. After the run the cell was rinsed several times by the solvent without disassembling it, both sectors were refilled with the solvent, and the cell was rerun for baseline corrections.

Low-speed equilibrium method[21] was used for all samples; the equilibrium concentration at the bottom of the cell was usually 3–4 times higher than the concentration at the top of the cell. The length of the liquid column was about 2.7 mm; the column length on the photograph was slightly less than 6 mm. Several attempts were made at the *high-speed equilibrium* method[22] with very low starting concentration. However, in all cases a severe convection prevented formation of a meaningful concentration profile. The convection was apparently caused by the inability of pure organic solvents to form a concentration and density gradient in the ultracentrifugal field and thus to stabilize the concentration pattern. (The high-speed method is used frequently for measurements of macromolecules of biological origin dissolved in buffered aqueous solution. The salts of the buffer provide the necessary stabilizing effect.) In low-speed experiments the concentration gradient of the polymer itself was enough to stabilize the run.

Initial concentration of the polymer solution must be known for the evaluation of the equilibrium photographs. It should be expressed in the same units as the concentration measured in the equilibrium photograph, i.e., in the fringe displacement, which, in turn, is measured either in units of length, y, or in number of fringes, f. These quantities are related to each other and to the concentration difference between the reference points, Δc, with the thickness of the liquid column, h, refractive index increment, $\Delta n/c$, and the wavelength of the light under vacuum, λ 5460 Å, by the following relations

$$f = (1/A)y = h\Delta n/\lambda = \Delta c(\Delta n/c)h/\lambda = B\Delta c \qquad (22)$$

Here, the conversion factor A depends on the optical alignment of the ultracentrifuge and typically has the value of about 0.290 mm/fringe. The conversion factor $B = f/\Delta c$ is evaluated from the synthetic boundary experiment described below, for which Δc is the known original concentration, c_0, expressed in g/ml.

Synthetic Boundary Experiment. The aluminum-filled-Epon synthetic boundary cell was filled with 0.15 ml of the same solution as used for the equilibrium run and with 0.44 ml of solvent. The rotor was brought to 4800 rpm and pictures taken for about 1.5–2 h. Then, the rotor with the cell was vigorously shaken to destroy all concentration gradients and a baseline correction run was made. The fringe count for the original solution, f_0, was evaluated by a method described previously.[13,23] In this method, the time dependence of the fringe count between two pairs of the reference points is used to find the correction for the possibly present solvent boundary. The method was slightly modified: both pairs of reference points were now fitted to a theoretical dependence simultaneously; this increased the reliability of the procedure. However, in the present experiments a single-component solvent was used; the solvent boundary, therefore, represented only low molecular weight impurities (such as moisture) and, indeed, was quite low in most cases. The average value of $\Delta n/c$ for polystyrene was 0.1024 ± 0.008 ml/g in benzene and 0.2219 ± 0.0012 ml/g in ethyl acetate. The conversion factor B was, accordingly, 2250 and 4877 fringe per g/ml for benzene and ethyl acetate.

Measurement and Evaluation of Interference Photographs for Equilibrium Experiments. The interference photographs were evaluated (cf. ref 14) on a Nikon profile projector equipped with a photomultiplier, logarithmic voltmeter, analog-to-digital converter and an X–Y stage operated by stepping motors. The projector was interfaced with a PDP-12 computer. Evaluation of each photograph was done in two parts. In the first part, the computer program instructed the operator to align the plate and to position the cross-hair successively on the reference wire, air fringes, the top and the bottom of the cell, and the first and last position in the column to be evaluated. The coordinates of these points were recorded by the computer. In the second, fully automated part of the program, the plate was scanned across the fringe pattern. The optical densities were analyzed by means of a Fourier transform using the algorithm described by DeRosier et al.[14] The following quantities were recorded for each scan: the radial position in the cell, the visibility of the fringe pattern, the displacement of the central fringe from the center of the scan, the distance between the center of the scan and the center of the envelope of the fringe band, and the fringe interval. The plate was scanned in intervals of 0.050 mm producing about 110 data points. For a typical equilibrium run three equilibrium photographs and one baseline photograph were evaluated; all the data were recorded on magnetic tape.

Analysis of the Equilibrium Data. The data on the magnetic tape recorded by the PDP-12 computer were then transferred to the CDC 6600/6400 computing system of the University of Texas. The computer program then processed the data in the following steps.

1. The points with inadequate visibility and any points judged unsatisfactory by the operator were deleted. In most cases, no points were deleted.

2. The residual tilt of the plate, due to unprecise alignment in the profile projector, was calculated from the reference air fringe positions and all the data were corrected for it.

3. There is an apparent discontinuity in the data when a new fringe is closest to the center of the scan. The discontinuity was removed by the addition of the fringe interval to the fringe displacement.

4. The x coordinates on the photographic plate were converted into radial distances in the sedimentation cell.

5. The fringe displacement on the baseline photograph was interpolated for the proper position on the solution column and subtracted from the equilibrium displacement.

6. The experimental dependence was extrapolated toward the top and the bottom of the liquid column by means of a quadratic calculated by a weighted least-squares method from respectively the first and last ten experimental points. The weighting method was similar to that described under step 9 below.

7. At this point, the concentration was expressed in the fringe displacement, y, on a scale, the arbitrary zero of which corresponds to some reference concentration y_{ref}. The reference concentration is calculated from the law of mass conservation which leads to the relation

$$y_{ref} = y_0 - 2\int_{r_t}^{r_b} yr\, dr/(r_b^2 - r_t^2) \qquad (23)$$

Here, y_0 is the original concentration of the solution measured in the synthetic boundary experiment and expressed in the units of fringe displacement. The radial distances of the top and the bottom of the liquid column are r_t and r_b, respectively. The part of the integral in eq 23 corresponding to the extrapolated dependences is calculated from the quadratic functions obtained in step 6 above. The main part of the integral is computed numerically from the experimental points using Simpson's rule. By addition of y_{ref} to values of y the data are converted to concentrations, y_{cor}.

8. The data are converted to the logarithms and for each point $d \ln y_{cor}/dr^2 \equiv (dc/dr)/2cr$ is calculated from the slope of the linear least-squares fit to experimental points. Eleven points bracketing the selected point are used for this fit. $1/M_{App}$ was calculated according to eq 12 (first identity) for each point.

9. The large number of closely spaced experimental points made it possible to smooth the data and to get less scattered dependences. After the data were smoothed, steps 6 through 8 were repeated. The smoothed dependence of $1/M_{App}$ on the concentration followed quite faithfully all the features of the unsmoothed dependence while reducing the scatter considerably. The algorithm of the smoothing procedure was as follows. For each experimental point nine (or less for points close to the end of the column) unsmoothed points bracketing the selected one were used for a linear least-squares fit in $\log y_{cor}$ vs. r^2 coordinates. Each point was assigned unit weight. Then, the deviation, Δ, of each point from the straight line was calculated and each point was assigned the weight $w = \exp(-(\Delta/\Delta_{st})^2)$. For the standard deviation, Δ_{st}, a value of 0.003 mm was used. The least-squares calculation was repeated, the weighing factors w were refined once more, and the least-squares fit repeated a third time. Then, the selected point was replaced by a point interpolated on the line. However, for the calculation of the refined value of the next point the unrefined point was still used. After all points were refined and replaced, the whole refining procedure was repeated once more. After the points were refined and replaced a second time, the program returned to step 6.

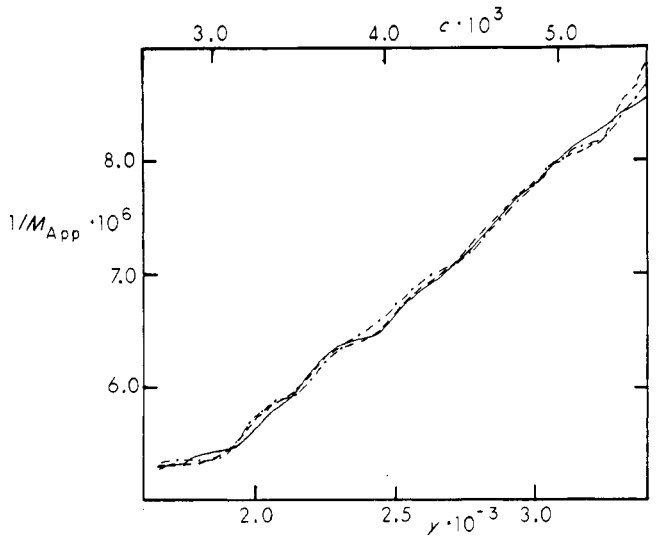

Figure 1. Plot of $1/M_{App}$ vs. concentration. Upper scale: c in g/ml; lower scale: y is fringe displacement in microns. Polystyrene **3b** (M = 379 000) in benzene: 20 °C, 5600 rpm. Different lines represent three equilibrium photographs taken 72 h after the start of the run.

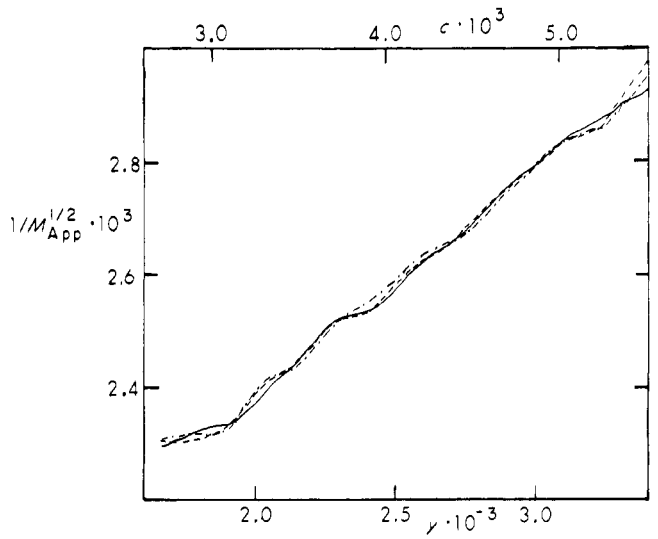

Figure 2. Plot of $1/M_{App}^{1/2}$ vs. concentration. Same data as in Figure 1.

10. The smoothed dependence $1/M_{App}$ vs. y_{cor} was plotted for all photographs in a single plot and the best straight line was drawn through the points. At this stage we preferred the hand-drawn line over the least-squares line drawn by the computer. However, in most cases the agreement between these two lines was quite close. The molecular weight and the second virial coefficient were calculated from the slope and intercept of the line and from the conversion factors A and B. The same treatment was used for the square-root plot $1/M_{App}^{1/2}$ vs. y_{cor}.

Results and Discussion

The typical experimental data for a highly nonideal sample of polystyrene **3b** in benzene are plotted in Figures 1 and 2 as respectively $1/M_{App}$ vs. c and $1/M_{App}^{1/2}$ vs. c. The plots represent the evaluation of three different equilibrium photographs (different types of line). Each line consists of over 100 smoothed experimental points; the individual points were connected by a straight line segment. The irregularities on the lines account for about 1% of the plotted quantity, 2–3% in regions close to the top and the bottom of the cell. The irregularities are quite reproducible for two readings of the same photograph; sometimes they are even similar for different photographs. In our opinion, they represent experimental

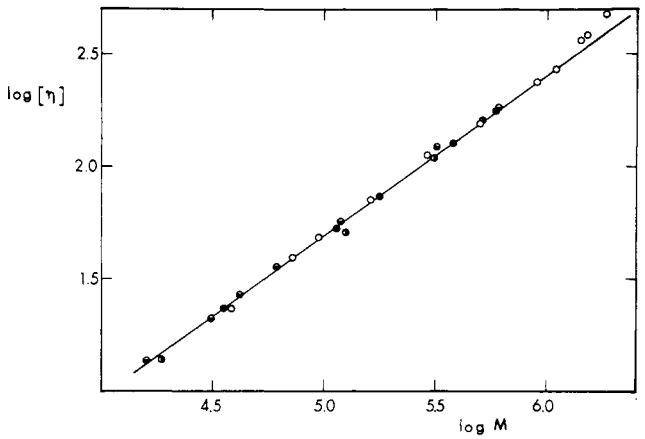

Figure 3. Dependence of intrinsic viscosity of benzene solutions of polystyrene on its molecular weight. (●) 20 °C, present data; (○) 25 °C, Bawn et al.;[24] (⊖) 25 °C, Krigbaum and Flory;[25] (◑) Meyerhoff.[26] The straight line represents eq 24.

error connected with cell and optics imperfections as well as the disturbances of the sedimentation equilibrium. They are not caused by the evaluation procedure. The photographic noise is virtually eliminated by the smoothing procedure.

It is obvious that *both* plots may be very well approximated by a straight line even for this highly nonideal system. It follows that the apparent linearity of the plot cannot be used as the criterion of the usefulness of the respective plots. The whole set of experimental data must be used for the evaluation.

The viscosity–molecular weight data of several authors[24–26] for polystyrene fractions in benzene are collected in Figure 3. The present data evaluated by the square-root plot for benzene solutions are included. In our opinion, the combined data are described best by the relation given by Meyerhoff[26]

$$[\eta] = 1.23 \times 10^{-2} M^{0.72} \quad (24)$$

The molecular weights of our samples calculated from their viscosities according to eq 24 are presented in Table I; they differ slightly from the manufacturer's values.

Sedimentation equilibria of ethyl acetate solutions yielded very similar molecular weights when evaluated either by means of the linear plot or the square-root plot (Table I). As expected, the linear plot yielded molecular weights slightly higher than the square-root plot, but the difference was within experimental error. The molecular weights agree quite closely with the values estimated from the intrinsic viscosity. Thus, the sedimentation method yields reasonable molecular weights when used with slightly nonideal solutions. Both the linear and square-root plot yield acceptable results.

Equilibria of highly nonideal benzene solutions yielded essentially the same molecular weights as above when evaluated by the means of the square-root plot (Table I). The values obtained from the linear plot were substantially higher; the difference between both sets of values increased with increasing molecular weight. Only for the highest molecular weight sample **13a** was the curvature of the $1/M_{App}$ vs. c plot pronounced enough to cause an a priori doubt about the linearity of the plot. Thus, for highly nonideal solutions the sedimentation method yields reasonable molecular weights only when the square-root plot is employed.

The construction of the linear plot was based on the assumption that the third virial term is negligible; that is equivalent to the assumption that $g = 0$. The square-root plot is based on assumption that $g = \frac{1}{3}$. The nature of the factor g is still not well-understood. According to Stockmayer and Casassa[16] g is an increasing function of the molecular expan-

Table I
Intrinsic Viscosities and Molecular Weights Measured by Sedimentation Equilibrium (Polystyrene)

Sample	η,[a] ml/g	M[b]	M_η[c]	M(benzene) Linear plot	M(benzene) Square-root plot	M(ethyl acetate) Linear plot	M(ethyl acetate) Square-root plot
7b	23.25	37 000	35 500	39 600	37 800	37 900	37 900
4b	52.4	110 000	109 900	121 300	113 000	116 900	116 600
1c	73.2	200 000	174 800	206 000	177 000	196 000	195 000
3b	126.7	390 000	374 500	656 000	379 000	383 000	377 000
13a	179.4	670 000	607 000	1 322 000	619 000	614 000	598 000

[a] In benzene, 20 °C. [b] Molecular weight claimed by the manufacturer. [c] From intrinsic viscosity, according to eq 24.

Table II
Second Virial Coefficient of Polystyrene Measured by Sedimentation Equilibrium

Sample	A_2(benzene) $\times 10^4$ Linear plot	A_2(benzene) $\times 10^4$ Square-root plot	A_2(ethyl acetate) $\times 10^4$ Linear plot	A_2(ethyl acetate) $\times 10^4$ Square-root plot	$\Delta A_2 \times 10^4$ [a]
7b	9.3	7.7	1.42	1.39	−1.32
4b	6.5	5.1	0.86	0.82	−0.53
1c	6.3	4.6	0.91	0.85	−0.38
3b	6.4	3.9	0.93	0.82	−0.33
13a	5.8	3.25	0.87	0.74	−0.30

[a] Error due to heterogeneity estimated from eq 18 and manufacturer's data.

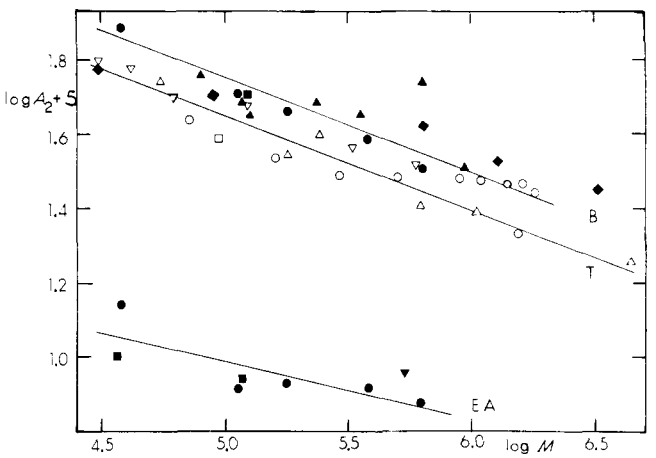

Figure 4. Dependence of second virial coefficient of polystyrene solutions. Benzene and ethyl acetate, full symbols; toluene, open symbols. (●) 20 °C, present data; (▲) IUPAC report;[27] (■) 25 °C, Vink;[30] (▼) 27 °C, Schick et al.;[29] (♦) Tager and Andreeva;[28] (○) 25 °C, Bawn et al.;[31] (△) 12 °C, Berry;[20] (▽) 30 °C, Krigbaum and Flory.[32] Interpolated lines: B benzene, T toluene, EA ethyl acetate.

sion and thus of molecular weight. For highly nonideal solutions the two plots yielded considerably different molecular weights; would then another choice of g yield still other results? According to Krigbaum and Flory,[17] the important thing is to take the third virial coefficient in account at all. If a wrong value of g is selected then the second virial coefficient will be overestimated and the third underestimated or vice versa. However, the effect on the first term (molecular weight) will be very small. Moreover, for small nonidealities, where the value of g is allegedly small, both linear and square-root plots yield almost identical results; for high nonidealities, the choice $g = \frac{1}{3}$ seems to be quite reasonable.

The second virial coefficients of our samples dissolved respectively in benzene and ethyl acetate are presented in Table II. In view of the above discussion, only the values obtained from the square-root plot are considered to be significant. In the last column of Table II an estimate of the error is presented, which is a result of the polydispersity of the sample according to eq 18. The values of the error were estimated using the manufacturer's data of $\bar{M}_w/\bar{M}_n$ assuming that $\bar{M}_z/\bar{M}_w \approx \bar{M}_w/\bar{M}_n$. According to the estimate, the error is about 10% for a good solvent, benzene; for a moderately good solvent, ethyl acetate, the relative error is more significant.

In Figure 4 our virial coefficients are plotted in a bilogarithmic plot as a function of molecular weight together with data found in the literature.[27-30] For comparison, the virial coefficients of polystyrene in toluene measured by several authors[20,31,32] are also included in Figure 4. The agreement between the present data and the literature data is reasonably good within a rather large experimental error. It should be mentioned, however, that the Schick et al. data[29] as well as the data from the IUPAC report[27] were measured on unfractionated samples of radically polymerized polystyrene. The values from the IUPAC report[27] plotted in Figure 4 are actually averages from several values given by different investigators. The virial coefficients seem to be slightly lower for toluene solutions than for benzene solutions; this corresponds well with the finding of Bawn et al.[24] that the intrinsic viscosity of the same sample of polystyrene is lower in toluene than in benzene. The virial coefficients in ethyl acetate solutions agree rather closely with the literature values.[29,30] (It should be noted that the Schick's value[29] corresponds to 27 °C and the Vink's value[30] to 25 °C. As the theta temperature for polystyrene in ethyl acetate is approximately −39 °C, we may estimate that their values would be lower by 5–10% at 20 °C.) The fact, that our virial coefficients for ethyl acetate solutions are not lower, but possibly are even higher than the reference data, may suggest that the errors listed in the last column of Table II are overestimated.

To test the possible effect of the redistribution of the polymer on the experimental results we have performed the sedimentation equilibrium experiment on the highest molecular weight sample **13a** at several rotor velocities between 3400 and 9000 rpm. All experimental dependencies superimposed within an experimental error. When the straight lines were drawn separately for each run the measured molecular weight and second virial coefficient were within 5% range. In another series of experiments[33] we measured the sedimentation equilibrium of the same samples in benzene at high concentrations and high rotor velocities under conditions where the region near meniscus was almost depleted of polymer. Under such conditions, the redistribution of molecular weights could be rather extensive and the proposed method may seem rather doubtful. Nevertheless, the experimental data superimposed almost exactly on the data reported above for samples **7b, 4b,** and **3b.** Only the more heterogeneous high molecular sample **13a** yielded molecular weight about 25% too

low while the virial coefficient remained the same as before. Such behavior suggests that large nonideality extensively suppresses the effects of heterogeneity as was expected from eq 15. Thus, the applicable limits of the method may be broader than suggested above.

Conclusions

The experimental data from sedimentation equilibrium in a single equilibrium run may be expressed as an apparent molecular weight, M_{App}, which is a function of the concentration of the solute, which, in turn, depends on the radial distance. Two methods are proposed for evaluation of the experimental dependences: (1) a plot of $1/M_{App}$ vs. c and (2) a plot of $1/M_{App}^{1/2}$ vs. c. In both cases the intercept of the straight line through the experimental points yields the molecular weight; the slope yields the second virial coefficient.

For ethyl acetate solutions of polystyrene, which represent moderately nonideal mixtures, both methods yield reasonable molecular weights. For highly nonideal benzene solutions of polystyrene only the square-root plot (2) yields reasonable values of molecular weight; a linear plot (1) yields too high a value.

For narrow fractions of the polymer, such as those used in this study, the method yields values of virial coefficient which are comparable to values obtained by osmometry and light scattering. However, the theoretical analysis predicts, that for polydisperse polymers the method will yield virial coefficients which are too low. Thus, caution is recommended when polymers are studied, which have a broader distribution of molecular weights.

Acknowledgment. The authors are grateful to the Robert A. Welch Foundation (Grant F-563) for financial support of this work.

References and Notes

(1) D. E. Roark and D. A. Yphantis, *Ann. N.Y. Acad. Sci.*, **164,** 245 (1969).
(2) V. L. Seery, E. H. Fisher, and D. C. Teller, *Biochemistry*, **6,** 3315 (1967); **9,** 3591 (1970).
(3) R. W. Green and R. H. McKay, *J. Biol. Chem.*, **244,** 5034 (1969).
(4) T. H. Donnelly, *J. Phys. Chem.*, **70,** 1862 (1966); *Ann. N.Y. Acad. Sci.*, **164,** 147 (1969).
(5) M. Gehatia and D. R. Wiff, *Adv. Chem. Ser.*, **No. 125,** 216 (1973).
(6) Th. G. Scholte, *J. Polym. Sci., Part A-2,* **6,** 91 (1968).
(7) Th. G. Scholte, *J. Polym. Sci, Part A-2,* **6,** 111 (1968).
(8) H. Fujita, "Foundations of Ultracentrifugal Analysis", Wiley, New York, N.Y., 1975.
(9) E. T. Adams, Jr., P. J. Wan, D. A. Soucek, and G. H. Barlow, *Adv. Chem. Ser.*, **No. 125,** 235 (1973).
(10) D. A. Albright and J. W. Williams, *J. Phys. Chem.*, **71,** 2780 (1967).
(11) R. C. Deonier and J. W. Williams, *Proc. Natl. Acad. Sci. U.S.A.*, **64,** 828 (1969).
(12) H. Utiyana, N. Tagata, and M. Kurata, *J. Phys. Chem.*, **73,** 1448 (1969).
(13) P. Munk and D. J. Cox, *Biochemistry*, **11,** 687 (1972).
(14) D. J. DeRosier, P. Munk, and D. J. Cox, *Anal. Biochem.*, **50,** 139 (1972).
(15) R. J. Goldberg, *J. Phys. Chem.*, **57,** 194 (1953).
(16) W. H. Stockmayer and E. F. Casassa, *J. Chem. Phys.*, **20,** 1560 (1952).
(17) W. R. Krigbaum and P. J. Flory, *J. Am. Chem. Soc.*, **75,** 1775 (1953).
(18) See Flory, ref 19, p 280.
(19) P. J. Flory, "Principles of Polymer Chemistry", Cornell University Press, Ithaca, N.Y., 1953.
(20) G. C. Berry, *J. Chem. Phys.*, **44,** 4550 (1966).
(21) E. G. Richards and H. K. Schachman, *J. Phys. Chem.*, **63,** 1578 (1959).
(22) D. A. Yphantis, *Biochemistry*, **3,** 297 (1964).
(23) P. Munk, R. G. Allen, and M. E. Halbrook, *J. Polym. Sci., Polym. Symp.*, **No. 42,** 1013 (1973).
(24) C. E. H. Bawn, R. F. J. Freeman, and A. R. Kamaliddin, *Trans. Faraday Soc.*, **46,** 1107 (1950).
(25) W. R. Krigbaum and P. J. Flory, *J. Polym. Sci.*, **11,** 37 (1953).
(26) G. Meyerhoff, *Z. Phys. Chem. (Frankfurt am Main)*, **4,** 335 (1955).
(27) H. P. Frank and H. Mark, *J. Polym. Sci.*, **10,** 129 (1952).
(28) A. A. Tager and V. M. Andreeva, *J. Polym. Sci., Part C,* **16,** 1145 (1967).
(29) M. J. Schick, P. Doty, and B. H. Zimm, *J. Am. Chem. Soc.*, **72,** 530 (1950).
(30) H. Vink, *Eur. Polym. J.*, **10,** 149 (1974).
(31) C. E. H. Bawn, R. F. J. Freeman, and A. R. Kamaliddin, *Trans. Faraday Soc.*, **46,** 862 (1950).
(32) W. R. Krigbaum and P. J. Flory, *J. Am. Chem. Soc.*, **75,** 1775 (1953).
(33) S. G. Chu and P. Munk, to be published.

Polymers in Mixed Solvents

J. Pouchlý[1a] and D. Patterson* [1b]

Institute of Macromolecular Chemistry, Czechoslovak Academy of Sciences, Prague 6, Czechoslovakia, and Department of Chemistry, McGill University, Montreal, P.Q., Canada H3C 3G1. *Received December 11, 1975*

ABSTRACT: A large discrepancy exists between published experimental values and theoretical predictions of heats of mixing of polymers to infinite dilution in mixed solvents. An even larger error exists for polymer intrinsic viscosities in mixed solvents. The predictions were made on the basis of the Flory–Huggins lattice model theory. We derive expressions using the more recent Prigogine–Flory theory which considers interactions to occur between molecular surfaces, and which is thus sensitive to the molecular surface/volume ratios of the polymer and solvent molecules. The theory also allows for thermodynamic effects associated with volume changes occurring during the mixing process. Both of these changes in theory are important when mixed solvents are used, and the new predictions are very different from those made with the Flory–Huggins theory. They are in good agreement with experiment for a number of systems with varied molecular surface/volume ratios.

A number of conveniently measured quantities may be used to investigate the interaction of a polymer (component 3) with mixed solvents (components 1 and 2), e.g., the heat of mixing of the polymer to infinite dilution,[2] its intrinsic viscosity,[3,4] or the swelling factor of the cross-linked polymer.[4,5a] These quantities reflect the (1–2) as well as the (1–3) and (2–3) interactions. Thus, the Flory–Huggins theory leads[2] to the following expression for the heat, L, absorbed on dissolving 1 g of polymer in an infinite amount of mixed-solvent of composition φ_1 (volume fraction):

$$L = (zv_3/v)(\varphi_1 w_{H_{13}} + \varphi_2 w_{H_{23}} - \varphi_1\varphi_2 w_{H_{12}}) \quad (1)$$

Here z is the lattice coordination number, v_3 is the specific volume of the polymer, v is the volume of a segment, and the $w_{H_{ij}}$ are the contact interchange energies. It is convenient to define a quantity ΔL representing the deviation of L from a linear interpolation between the values in the pure solvents, L_1 and L_2. Equation 1 predicts[2] that ΔL reflects only the (1–2) interaction:

$$\Delta L \equiv L - (\varphi_1 L_1 + \varphi_2 L_2) = -z(v_3/v)\varphi_1\varphi_2 w_{H_{12}} = -\Delta H_{12}(\varphi_1) \quad (2)$$

Here $\Delta H_{12}(\varphi_1)$ is the heat of mixing the liquids 1 and 2 to form